COMMUNICATIONS CHEMISTRY

ARTICLE

DOI: 10.1038/s42004-018-0065-4 OPEN

Catalytic asymmetric synthesis of chiral trisubstituted heteroaromatic allenes from 1,3-enynes

Songjie Yu[1], Hui Leng Sang[1], Shuo-Qing Zhang[2], Xin Hong[2] & Shaozhong Ge[1]

Chiral allene and *N*-heteroaryl motifs are present in an ever-growing list of biologically active natural products and synthetic drugs. Although significant progress has been made in asymmetric syntheses of chiral allenes, general and practical protocols for enantioselective syntheses of chiral *N*-heteroaryl-substituted allenes from readily available starting materials still remain rare. Here we report a highly enantioselective synthesis of quinolinyl-substituted chiral allenes through a copper-catalyzed asymmetric allenylation of quinoline *N*-oxides with readily available 1,3-enynes. A variety of 1,3-enynes react with quinoline *N*-oxides, affording the corresponding quinolinyl-substituted allenes in high yields (up to 95%) and high enantioselectivities (up to 99% ee). This transformation tolerates a variety of functional groups, such as chloro, bromo, trifluoromethyl ether, tertiary amine, siloxy, carboxylic ester, imide, pyridine, and thiophene moieties. DFT calculations suggest a pathway involving an intramolecular nucleophilic addition of an allenyl copper intermediate with a coordinated quinoline *N*-oxide through a five-membered, rather than seven-membered, transition state.

[1] Department of Chemistry, National University of Singapore, 3 Science Drive 3, Singapore 117543, Singapore. [2] Department of Chemistry, Zhejiang University, Hangzhou 310027, P. R. China. Correspondence and requests for materials should be addressed to X.H. (email: hxchem@zju.edu.cn) or to S.G. (email: chmgsh@nus.edu.sg)

Chiral allene moieties are present in a variety of natural products, molecular materials, and a few marketed drugs due to their unique structural features, chemical reactivity, and biological properties[1,2]. In addition, chiral allenes also represent a class of useful starting materials for a variety of organic transformations[3]. Accordingly, substantial endeavors have been made to develop methodologies for the asymmetric synthesis of chiral allenes. Classic approaches typically involve (kinetic) resolution of racemic allenes[4,5] or chirality transfer from optically pure propargylic precursors[6–10]. Recent years have witnessed a tremendous development on metal-catalyzed enantioselective synthesis of chiral allenes[11–16], such as nucleophilic addition to 1,3-enynes[17–19], enantioselective functionalization of racemic allenes[20–22], β-hydride elimination from enol triflates[23], rearrangement of propargylic compounds[24–27], coupling of terminal alkynes with diazo compounds[28–31], and enantioselective addition of terminal alkynes to aldehydes[32]. In addition, several asymmetric organocatalytic protocols have also been reported, such as nucleophilic addition to activated enynes[33,34], isomerization of alkynes[35,36], phase-transfer-catalyzed alleno-Mannich reaction[37,38], alkynylogous Mukaiyama aldol reactions[39], and chiral ion-pair catalysis involving a formal propargylic carbocation from racemic propargylic alcohols[40]. Notwithstanding these significant advances, asymmetric synthesis of chiral allenes, particularly *N*-heteroaryl-substituted chiral allenes[36], from readily available starting materials is particularly important and still remains a highly challenging task.

Chiral functionalized quinoline motifs are found in numerous biologically and pharmaceutically active alkaloids[41]. In addition, chiral quinoline is also a privileged scaffold for cinchonidine-type organocatalysts[42] and ligands for transition metal catalysis[43]. In view of the importance of functionalized quinolines and the importance of chiral allenes, we are interested in developing a general, enantioselective protocol for the asymmetric synthesis of quinoline-substituted chiral allenes. Furthermore, quinoline-substituted allenes, which are important but synthetically challenging, are unprecedented to the best of our knowledge.

1,3-Enynes can be readily prepared via Sonogashira coupling reactions[44], and are valuable potential precursors to access allenes. However, known synthetic methods to make chiral allenes from 1,3-enynes are rather limited to reactions of activated or electron-deficient 1,3-enynes[17–19,33,34], and non-activated 1,3-enynes do not undergo these nucleophilic addition reactions due to their weak electrophilicity. Recent advances on Cu-catalyzed functionalization of alkenes indicate successful conversions of alkenes to nucleophilic alkylcopper species[45–54]. Furthermore, Cu-catalyzed functionalization of 1,3-enynes has also been studied (Fig. 1a)[55,56]. For example, Hoveyda reported a nucleophilic addition to aldehydes with nucleophiles generated from a borylcopper species and 1,3-enynes[55]. In 2016, Buchwald and Liu reported an asymmetric addition to ketones using nucleophiles derived from migratory insertion of 1,3-enynes to a chiral Cu-H intermediate[56]. Both reactions provide propargylic products selectively (Fig. 1a)[55,56], although density functional theory (DFT)-calculation studies suggest a facile isomerization of initially generated propargylic copper species to allenyl copper intermediates during conversions of 1,3-enynes. Very recently, Hoveyda, Engle, and Ge groups have independently reported enantioselective copper-catalyzed hydroboration of 1,3-enynes through trapping of allenyl copper species with pinacolborane (Fig. 1b)[57–60].

We recently reported an asymmetric alkylation of quinoline *N*-oxides with chiral alkylcopper species[60]. Inspired by the suitability of quinoline *N*-oxides as electrophiles for alkylcopper nucleophiles, we envisioned that quinoline *N*-oxides could serve as proper electrophiles to react with allenyl copper species to form chiral allene products through a five-membered, rather than seven-membered, transition state (Fig. 1c). Herein, we report our studies toward the development of an enantioselective synthesis of quinolinyl-containing chiral allenes.

Results

Evaluation of reaction conditions. We began our studies on this asymmetric allenylation by identifying an effective and selective chiral copper catalyst for the reaction between but-3-en-1-yn-1-ylbenzene (**2a**) and quinoline *N*-oxide (**1a**). We tested copper complexes generated in situ from CuOAc and various chiral bisphosphine ligands as catalysts. The results are summarized in Fig. 2. These reactions were conducted with $(EtO)_2MeSiH$ as hydride source in cyclohexane at 5 °C for 20 h, and the allene **3a** was identified as a major product for these reactions. The reaction catalyzed by the combination of CuOAc and (*R*)-DTBM-segphos (**L1**) occurred smoothly and afforded **3a** in good yield (74%), but with modest enantioselectivity (46%). Similar results were obtained for the reactions when catalysts generated from CuOAc and chiral ligands **L2**–**L5** were employed. However, the reaction conducted with CuOAc and (*S*,*S*)-Ph-BPE (**L6**) produced **3a** in high isolated yield (90%) with excellent enantioselectivity (95%). In addition, we also studied other reaction parameters, such as solvents, temperature, and hydride sources, and found that the reactions afforded the desired product **3a** either in lower yields or with lower enantioselectivities under these tested conditions (for the details, see Table S1).

Scope of 1,3-enynes for Cu-catalyzed enantioselective allenylation of quinoline *N*-oxide. With an active chiral copper catalyst and reliable conditions identified, we studied the scope of alkyl-substituted 1,3-enynes for this Cu-catalyzed asymmetric allenylation, and the results are summarized in Fig. 3. In general, a

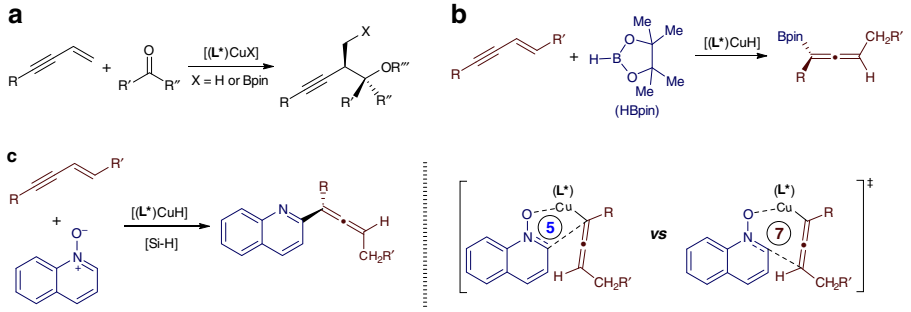

Fig. 1 Copper-catalyzed enantioselective hydrofunctionalization of 1,3-enynes. **a** Trapping allenyl copper intermediates with carbonyls to form propargylic products. **b** Copper-catalyzed asymmetric hydroboration of 1,3-enynes. **c** This work: trapping allenyl copper intermediates with quinoline *N*-oxide

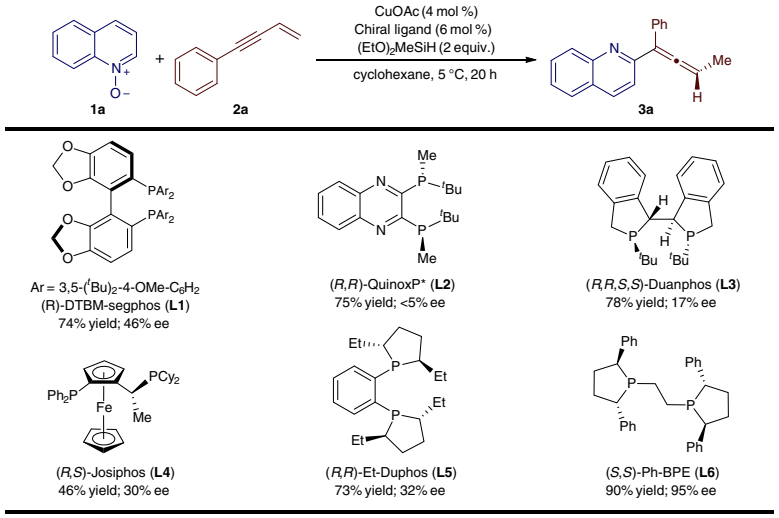

Fig. 2 Evaluation of ligands for this copper-catalyzed chiral allene synthesis. Reaction conditions: quinoline *N*-oxide **1a** (0.400 mmol), but-3-en-1-yn-1-ylbenzene **2a** (0.200 mmol), $(EtO)_2MeSiH$ (0.400 mmol), CuOAc (8.0 μmol), ligand (12.0 μmol), cyclohexane (1 mL), 5 °C, 20 h, isolated yield, and ee was determined by chiral HPLC analysis

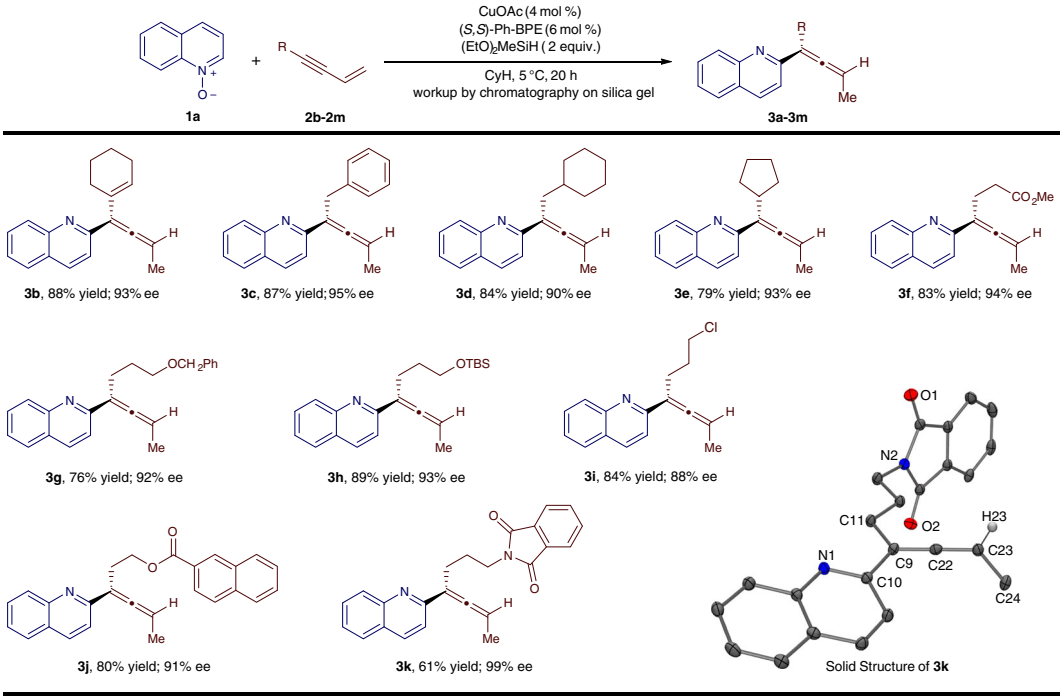

Fig. 3 Scope of aliphatic-substituted 1,3-enynes. Reaction conditions: quinoline *N*-oxide **1a** (0.400 mmol), enyne (0.200 mmol), $(EtO)_2MeSiH$ (0.400 mmol), CuOAc (8.0 μmol), (*S*,*S*)-Ph-BPE (12.0 μmol), cyclohexane (1 mL), 5 °C, 20 h, isolated yields, and ee was determined by chiral HPLC analysis

variety of alkenyl- or alkyl-substituted 1,3-enynes (**2b**–**2k**) smoothly underwent this Cu-catalyzed enantioselective transformation to afford the corresponding allene products (**3b**–**3k**) in high isolated yields (61−89%) with good to excellent enantioselectivities (88–99%). Enynes bearing reactive groups, such as ester (**3f** and **3j**), benzyl ether (**3g**), siloxy (**3h**), and imide (**3k**), are compatible with the reaction conditions. The absolute configuration of **3k** was assigned as (*S*) by single-crystal X-ray diffraction (XRD) analysis.

The scope of aryl-substituted 1,3-enynes for this reaction is summarized in Fig. 4. In general, a wide range of aryl-substituted 1,3-enynes reacted under standard condition to produce the corresponding allene products (**3l**–**3ag**) in high yields (70−95%) and with high enantioselectivities (80–96%). The data in Fig. 4 indicate that the electronic properties of the aryl groups in aryl-substituted enynes have noticeable influence on the enantioselectivity of this reaction. For example, enynes containing electron-neutral and electron-rich aryl groups reacted to afford allenes **3a** and **3l**–**3n** with high enantioselectivities (90–94%), but the reactions of enynes containing electron-deficient aryl groups (**2q**–**2s**) took place with lower enantioselectivities (80–83% for **3q**–**3s**). The steric hindrance at the *para*- or *meta*-positions of the aryl groups in aryl-substituted enynes has little effect on the enantioselectivity of this transformation (90–94% ee for **3l**–**3o**).

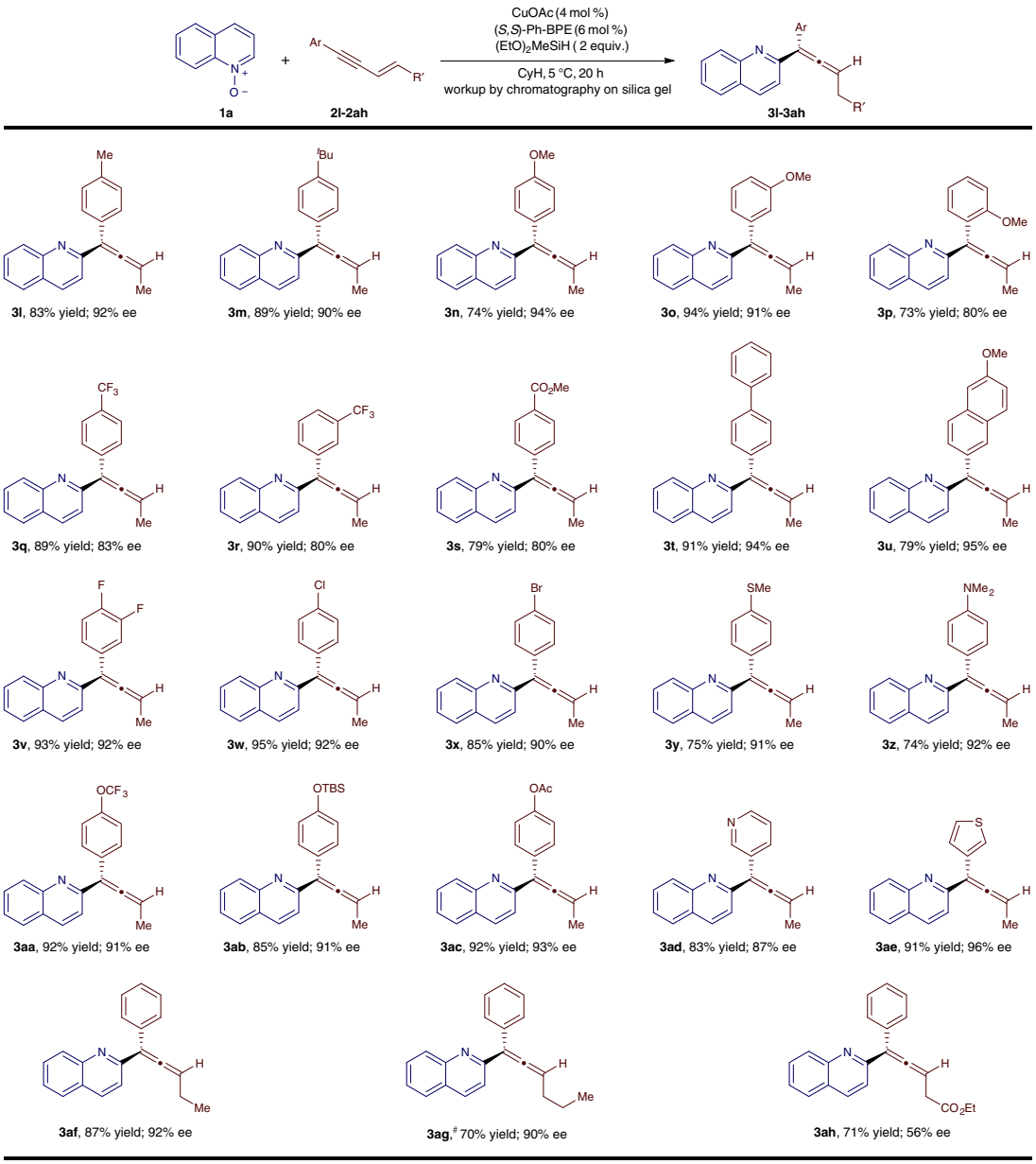

Fig. 4 Scope of aromatic-substituted 1,3-enynes. Reaction conditions: quinoline *N*-oxide (0.400 mmol), enyne (0.200 mmol), $(EtO)_2MeSiH$ (0.400 mmol), CuOAc (8.0 μmol), (*S*,*S*)-Ph-BPE (12.0 μmol), cyclohexane (1 mL), 5 °C, 20 h, isolated yields, and ee was determined by chiral HPLC analysis. #CuOAc (16.0 μmol), (*S*,*S*)-Ph-BPE (24.0 μmol)

However, the reaction of an enyne containing *ortho*-substituted aryl group (**2p**) occurred with significantly lower enantioselectivity (80% ee for **3p**).

This Cu-catalyzed asymmetric transformation tolerates a range of functionalities, including fluoro (**3v**), chloro (**3w**), bromo (**3x**), thioether (**3y**), tertiary amine (**3z**), trifluoromethyl ether (**3aa**), silylether (**3ab**), and carboxylic ester (**3s**, **3ac**, and **3ah**) moieties. 1,3-Enynes bearing nitrogen- and sulfur-containing heteroaryl substituents also reacted to produce the corresponding allenes (**3ad** and **3ae**) in high yields and high enantioselectivity. In addition, 1,3-enynes with substitution at the olefenic terminus of the enynes ((*Z*)-**2af** and (*Z*)-**2ag**) also reacted to afford the corresponding allenes (**3af** and **3ag**) in high isolated yields and good enantioselectivities. (*Z*)-2-Alken-4-ynoate (**2ah**), an activated 1,3-enyne, also reacted to give the allene product **3ah** in high yield, albeit with a modest enantioselectivity. However, (*Z*)-oct-2-en-4-yne, a 1,3-enyne containing two alkyl groups at 1,4-positions, does not undergo this Cu-catalyzed asymmetric reaction.

Scope of quinoline *N*-oxides. Fig. 5 summarizes the scope of quinoline *N*-oxides for this Cu-catalyzed asymmetric allenylation transformation. In general, quinoline *N*-oxides with substituents at various positions reacted smoothly with the enyne **2a** to yield the corresponding allenes (**3ai**–**3ar**) in high yields and high enantioselectivities. However, 8-methyl and 8-methoxyquinoline *N*-oxides reacted with decreased enantioselectivities (**3as** and **3at**), which might be due to the increased steric hindrance around the N–O bond. Various reactive groups, such as chloro (**3am** and **3an**), bromo (**3ao** and **3ap**), siloxy (**3aq**), and carboxylic ester (**3ar**), at different positions of quinoline *N*-oxides were tolerated, and the allene products were isolated in high yields (61–97%) with high to excellent enantioselectivities (84–97% ee).

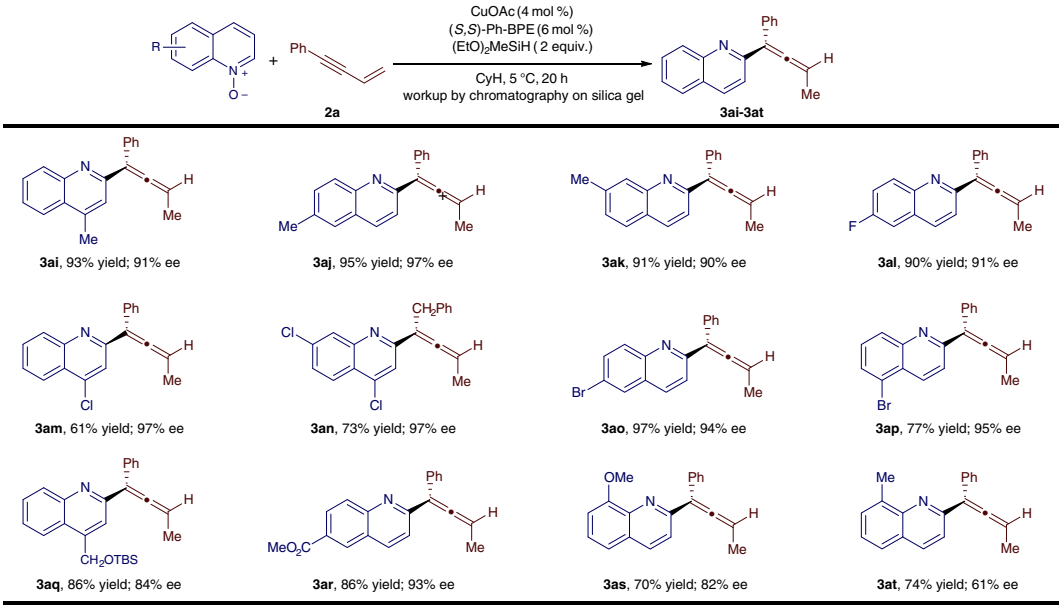

Fig. 5 Scope of quinoline *N*-oxides. Reaction conditions: quinoline *N*-oxide **1a** (0.400 mmol), enyne (0.200 mmol), $(EtO)_2MeSiH$ (0.400 mmol), CuOAc (8.0 μmol), (*S*,*S*)-Ph-BPE (12.0 μmol), cyclohexane (1 mL), 5 °C, 20 h, isolated yields, and ee was determined by chiral HPLC analysis

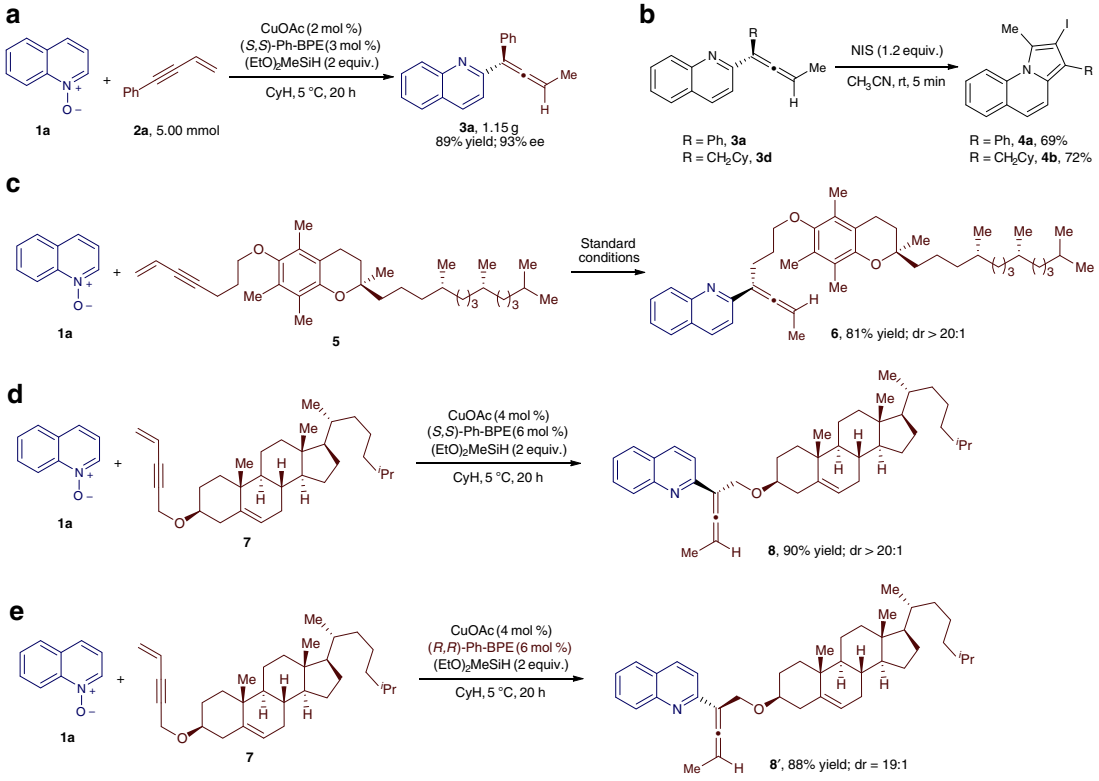

Fig. 6 Synthetic applications. **a** Gram-scale reaction. **b** NIS-promoted cyclization of quinoline-substituted allenes. **c**–**e** Allenylation reactions with chiral allenes derived from vitamin E and cholesterol. Yields are reported for isolated materials after column chromatography on silica gel

However, the allenylation reactions of *N*-oxides of pyridines and isoquinolines do not occur under identified conditions.

Synthetic potential. To show the utility of this asymmetric protocol, the reaction of quinoline *N*-oxide **1a** with enyne **2a** was conducted on gram scale with 2 mol% copper catalyst at 5 °C. This reaction proceeded to full conversion of **2a** in 20 h and afforded allene **3a** in 89% isolated yield and with 93% ee (Fig. 6a). The enantioselectivity of this gram-scale reaction is comparable to that of a 0.200 mmol scale reaction (Fig. 2). In addition, we also showed that the quinoline-substituted allene products **3a** and **3d** underwent NIS-initiated cyclization to generate the corresponding 2-iodo-pyrrolo[1,2-*a*]quinolones in good yields (Fig. 6b, NIS = *N*-iodosuccinimide)[61].

This copper-catalyzed asymmetric allenylation was utilized for the modification of complex molecules. For example,

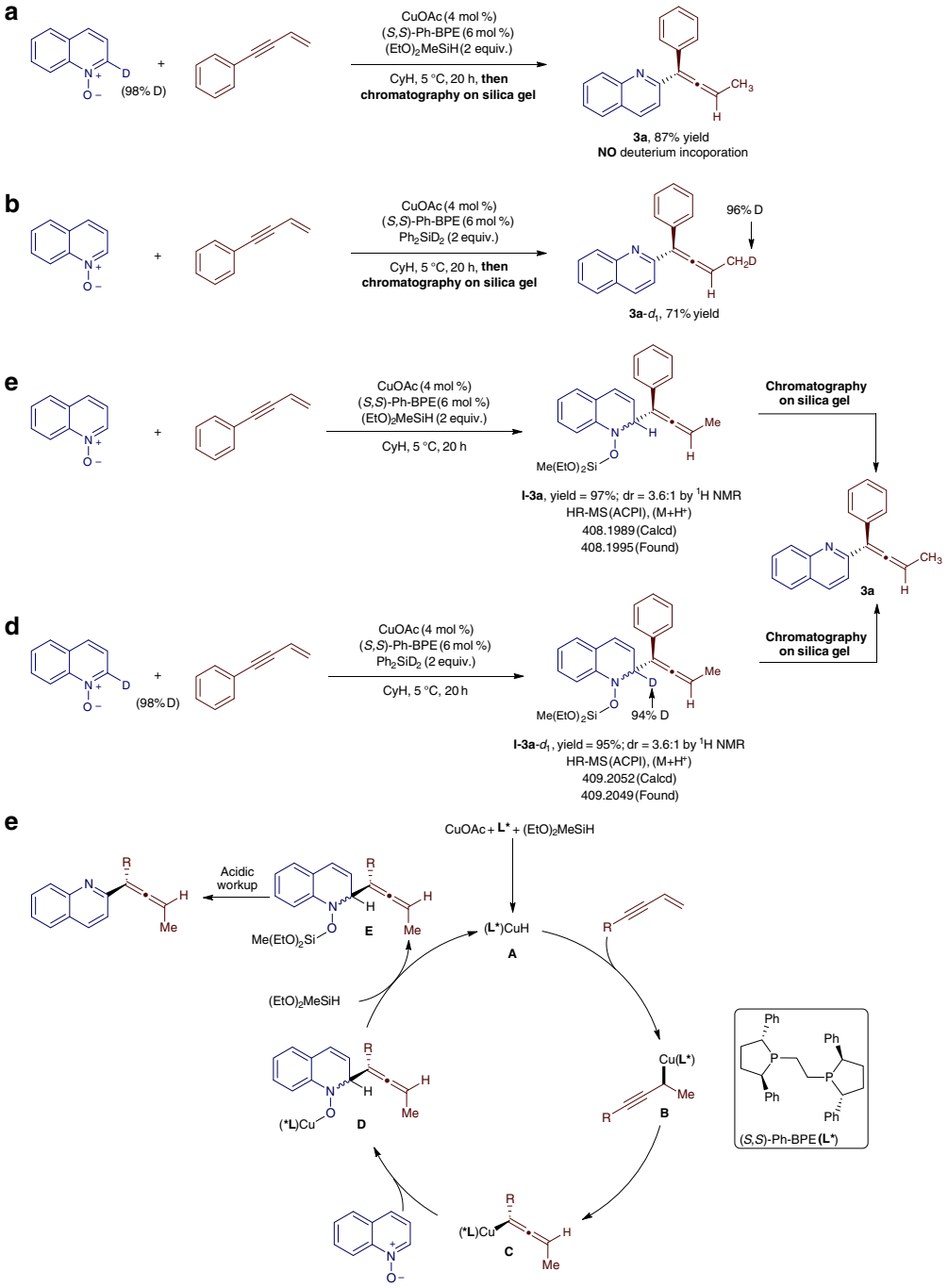

Fig. 7 Mechanistic studies. **a**–**d** Deuterium-labeling experiments. **e** Proposed catalytic pathway for this Cu-catalyzed asymmetric allenylation reaction

the allenylation of quinoline *N*-oxide **1a** with enantiometrically pure 1,3-enynes **5** and **7** (**5** derived from vitamin E and **7** derived from cholesterol, respectively) occurred smoothly in the presence of 4 mol% CuOAc/(*S*,*S*)-Ph-BPE, affording chiral allenes **6** and **8** in high isolated yields with excellent diastereoselectivity (dr > 20:1), respectively (Fig. 6c, d). The corresponding reaction with enyne **7** conducted with CuOAc/(*R*,*R*)-Ph-BPE produced the opposite diastereomers **8′** in comparable yield and with similarly high diastereoselectivity. The results of this experiment indicate a mechanism involving catalyst control rather than substrate control when enantiometrically pure 1,3-enynes are used. The absolute configuration of compounds **6**, **8**, and **8′** was assigned by analogy to that of compound **3k**.

Mechanistic considerations. To gain some mechanistic insights into this Cu-catalyzed asymmetric allenylation of quinoline *N*-oxides, we conducted a series of deuterium-labeling experiments (Fig. 7). The reaction of quinoline-2-*D* *N*-oxide **1a**-d_1 with 1,3-enyne **2a** under standard conditions afforded **3a** in high isolated yield after purification with flash chromatography on silica gel, but no deuterium was incorporated into the product (Fig. 7a). When conducted with Ph_2SiD_2, the reaction of quinoline *N*-oxide **1a** with 1,3-enyne **2a** produced **3a**-d_1 in high isolated yield after purification with flash chromatography on silica gel, and the deuterium was located in the methyl group of **3a** (Fig. 7b).

To detect the potential intermediates for this Cu-catalyzed asymmetric allenylation, we monitored by ^{1}H nuclear magnetic resonance (NMR) analysis the reaction of quinoline *N*-oxide **1a** and

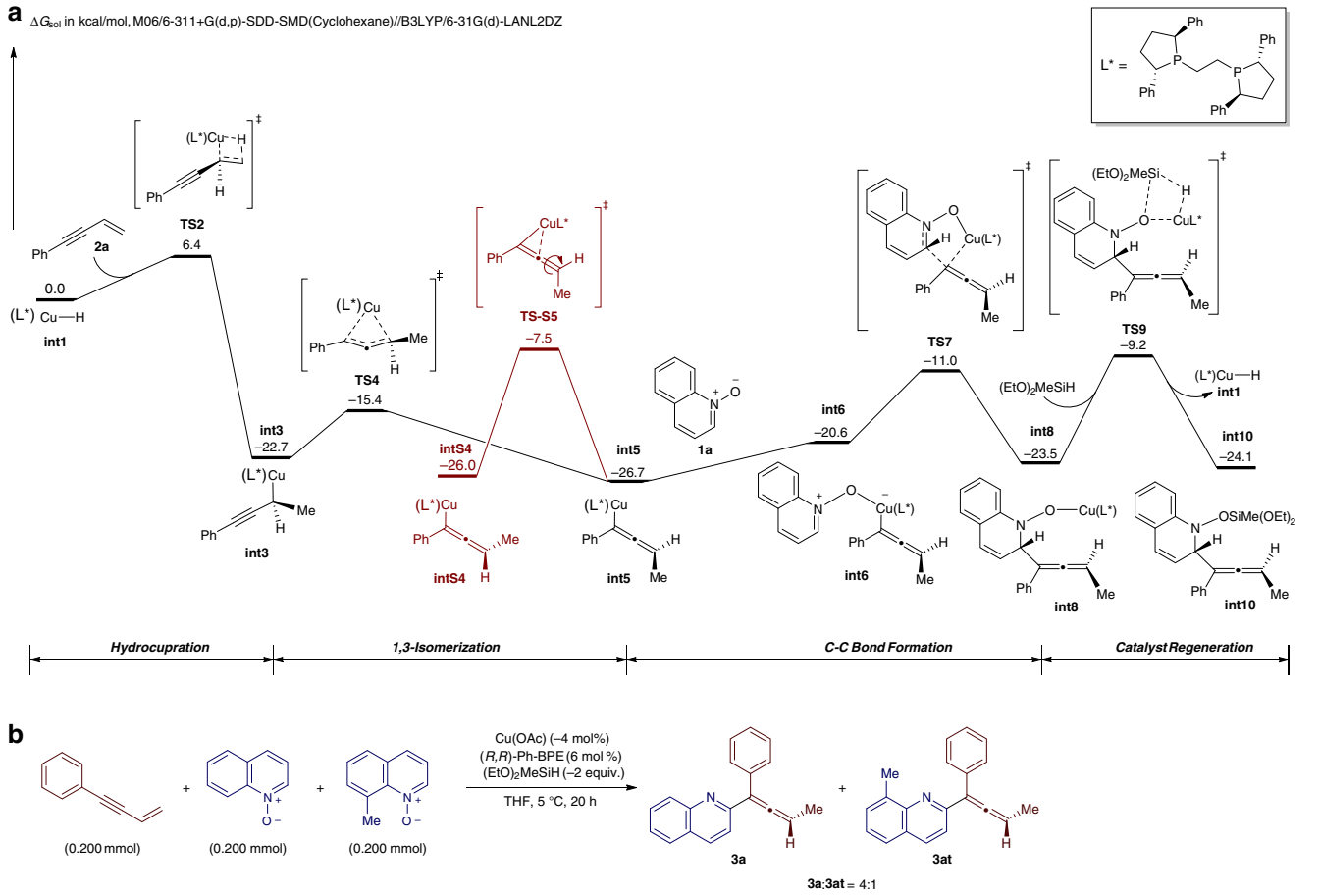

Fig. 8 DFT studies. **a** DFT-computed free energy changes of the most favorable pathway for the Cu-catalyzed enantioselective allenylation of quinoline *N*-oxide **1a** with 1,3-enyne **2a**. **b** A competition experiment between sterically differentiated quinoline *N*-oxides

enyne **2a** under standard conditions, and found that this reaction afforded **I-3a** with a modest diastereoselectivity (dr = 3.6:1) in high yield prior to the isolation of final product by flash choromatography on silica gel (Fig. 7c). Correspondingly, the reaction of quinoline-2-*D* *N*-oxide **1a**-d_1 with 1,3-enyne **2a** produced the intermediate **I-3a**-d_1 in 95% yield with a diastereoselectivity of 3.6:1 (Fig. 7d). Upon workup by column chromatography on silica gel, both intermediates **I-3a** and **I-3a**-d_1 underwent re-aromatization to yield 2-allenyl quinoline **3a** in high yields.

Based on the precedent of reactions of quinoline *N*-oxides with metal-alkyl reagents[62,63], the Cu-catalyzed hydrofunctionalization of 1,3-enynes[57–59], and the results of the above-mentioned mechanistic experiments, we proposed a plausible catalytic pathway for this Cu-catalyzed asymmetric allenylation of quinoline *N*-oxides (Fig. 7e). Activation of CuOAc with $(EtO)_2MeSiH$ in the presence of (*S*,*S*)-Ph-BPE (**L***) produces a chiral copper hydride species (**L***)Cu-H (**A**). Enantioselective migratory insertion of 1,3-enyne into (**L***)Cu-H forms a propargylic copper intermediate **B**, which then undergoes a stereospecific isomerization to an allenyl copper species **C**. This allenyl copper intermediate reacts with quinoline *N*-oxide to form a copper species **D**, which reacts with $(EtO)_2MeSiH$ to afford a siloxane intermediate **E** and to regenerate the catalytically active Cu-H species **A**. The siloxane intermediate **E** then aromatizes to form the 2-allenyl quinoline product.

DFT calculations. With DFT calculations, we explored the mechanism and origins of chemoselectivity based on the reaction of quinoline *N*-oxide **1a** and 1,3-enyne **2a** catalyzed by the combination of CuOAc and (*S*,*S*)-Ph-BPE. The computed free energy diagram of the most favorable pathway is shown in Fig. 8a (see Supplementary Figure 18 for the detailed calculations on other pathways). From the Cu-H species **int1**, the hydrocupration of **2a** occurs via **TS2** and generates the propargyl copper intermediate **int3** enantioselectively. The origins of this enantioselective hydrocupration step have been discussed, by Buchwald and Liu, for a Cu-catalyzed asymmetric addition of olefin-derived nucleophiles to ketones[51]. This hydrocupration step determines the enantioselectivity of this Cu-catalyzed allenylation reaction. From **int3**, the stereospecific 1,3-isomerization via **TS4** to form **int5** is facile. Thus, the propargyl copper species **int3** and the corresponding allenyl copper species **int5** are in a fast equilibrium. The final C–C bond formation proceeds through the five-membered ring transition state **TS7** leading to the intermediate **int8**. Further exchange with $(EtO)_2MeSiH$ affords **int9** and regenerates the Cu-H species **int1** for the next catalytic cycle. Based on the free energy changes of the whole catalytic cycle, the allenyl copper intermediate **int5** is the on-cycle resting state, and the rate-determining step is the regeneration of active catalyst **int1** via **TS9**, which is consistent with previous related experimental mechanistic results[64].

In addition, we also discovered an epimerization pathway from **int5** to **intS4** via **TS-S5** (depicted in Fig. 8a), which could be responsible for the varied enantioselectivities obtained for the reactions with different quinoline *N*-oxides (Fig. 5). For example, 8-methyl quinoline *N*-oxide reacted with a significantly lower enantioselectivity (61% ee for **3at** in Fig. 5) than quinoline *N*-oxide (95% ee for **3a** in Fig. 2). We attributed this decreased

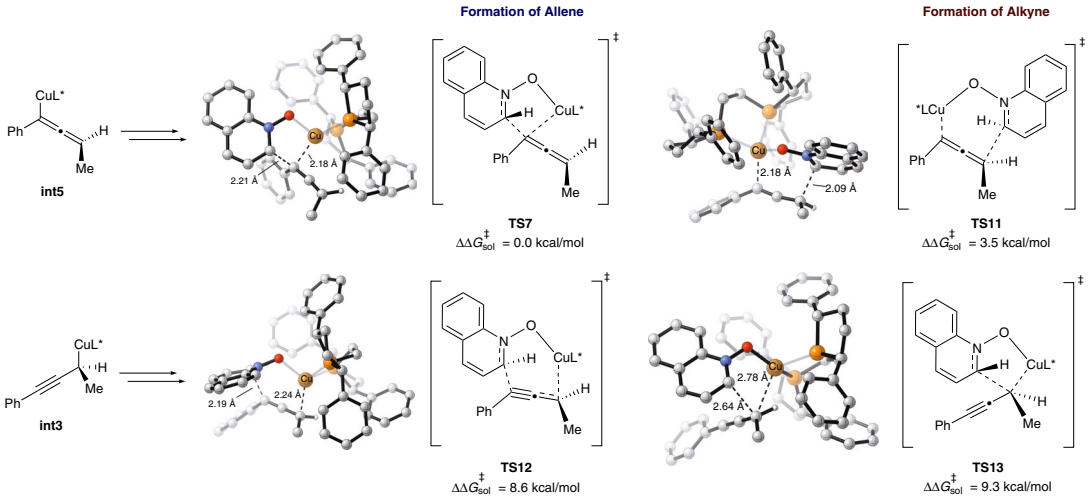

Fig. 9 Optimized structures and relative free energies of competing transition states for C–C bond formation

enantioselectivity to a slower rate for the reaction of 8-methyl quinoline *N*-oxide, caused by the increased steric hindrance around the N–O bond. To further prove the difference in reactivity, we conducted a competition experiment of 1,3-enyne **2a** between quinoline *N*-oxide and 8-methyl quinoline *N*-oxide in a single reaction vessel (Fig. 8b). Indeed, the allene product (**3av**) from the reaction of 8-methyl quinoline *N*-oxide was produced in a much smaller quantity than the product (**3a**) from the reaction of quinoline *N*-oxide.

The C–C bond formation step determines the chemoselectivity between allene and alkyne products. We carefully examined the possible transition states for the C–C bond formation, and the key competing ones are shown in Fig. 9. The propargyl copper intermediate **int3** is 4.0 kcal/mol unfavorable as compared to the allenyl copper intermediate **int5**. This thermodynamic difference also reflects in the corresponding transition states, and **TS12** and **TS13** (from **int3**) are less favorable than **TS7** and **TS11** (from **int5**). Comparing **TS7** and **TS11**, the calculations suggest a strong selectivity toward the formation of allene product via **TS7**, which is consistent with the experimental selectivity (Fig. 2). **TS7** is a five-membered ring transition state, while the competing **TS11** requires a seven-membered metallacycle, which is unfavorable due to the ring strain. The important role of metallacycle in determining the chemoselectivity provides insights for the reaction design with allenyl and propargyl copper species.

Discussion

In summary, we report an efficient and enantioselective protocol for the asymmetric synthesis of trisubstituted allenes through a Cu-catalyzed allenylation of quinoline *N*-oxides with 1,3-enynes. A wide range of aryl- and alkyl-substituted 1,3-enynes reacted with quinoline *N*-oxides to afford the corresponding allenes in high isolated yields with good to excellent enantioselectivity. This asymmetric transformation could be readily conducted on a gram scale with a reduced catalyst loading (2 mol%), and thus this protocol presents a practical route to prepare enantiomerically enriched quinoline-containing trisubstituted allenes from readily accessible quinoline *N*-oxides and 1,3-enynes. DFT calculations suggest that this Cu-catalyzed allenylation occurs through a nucleophilic attack of quinoline *N*-oxide with an allenyl copper intermediate via a five-membered transition state, thereby providing a rationale to explain the obtained chemoselectivity toward an allene rather than a propargylic product. These findings will enable future development of new reactions with an allenyl or a propargyl copper intermediate, and these studies will be the subject of future work.

Methods

General procedure for the synthesis of chiral allenes. CuOAc (4 mol%, 0.9 mg) and (*S*,*S*)-Ph-BPE (6 mol%, 6.1 mg) were dissolved in cyclohexane (1 mL) in a screw-capped vial under argon atmosphere. The resulting mixture was stirred for 5 min, to which was added (EtO)SiHMe (0.400 mmol, 65 μL), 1,3-enynes (0.200 mmol), and quinoline *N*-oxide (0.400 mmol) successively. The vial was stirred at 5 °C for 20 h. The mixture was concentrated under vacuum and the crude product was purified by flash chromatography on silica with a mixture of ethyl acetate/hexane (1:100 to 1:50). The ee values were determined by high-performance liquid chromatography.

(Note: The allene products are unstable and prone to racemization in acidic solvent such as $CHCl_3$. The ee values and optical rotation should be determined immediately after isolation.)

Mechanistic studies. Spectra pertaining to deuterium labeling, competition, and other mechanistic studies are available in Supplementary Figures 1-16.

Synthesis and characterization. Full synthetic procedures are available in the Supplementary Methods. The XRD structure of **3k** is available in Supplementary Figure 17 and Supplementary Data 1-2. NMR spectra of purified organic compounds are available in Supplementary Figures 19-128.

Screening conditions. Further details of reaction conditions screened are available in Supplementary Table 1.

Computational study. Full procedures and results are available in the Supplementary Methods, Supplementary Figure 18, and Supplementary Table 2. Cartesian coordinates of calculated intermediates and transition states are available in Supplementary Table 3.

Data availability

The authors declare that all data supporting the findings of this study are available within the article and Supplementary Information files, and also are available from the corresponding author upon reasonable request. The X-ray crystallographic coordinates for the structure reported in this article has been deposited at the Cambridge Crystallographic Data Centre (CCDC), under deposition number CCDC 1823673. These data can be obtained free of charge from The Cambridge Crystallographic Data Centre at www.ccdc.cam.ac.uk/data_request/cif.

Received: 12 May 2018 Accepted: 25 September 2018
Published online: 17 October 2018

References

1. Hoffmann-Röder, A. & Krause, N. Synthesis and properties of allenic natural products and pharmaceuticals. *Angew. Chem. Int. Ed.* **43**, 1196–1216 (2004).

2. Rivera-Fuentes, P. & Diederich, F. Allenes in molecular materials. *Angew. Chem. Int. Ed.* **51**, 2818–2828 (2012).
3. Krause, N. & Hashmi, A. S. K. *Modern Allene Chemistry* (Wiley, 2004).
4. Trost, B. M., Fandrick, D. R. & Dinh, D. C. Dynamic kinetic asymmetric allylic alkylations of allenes. *J. Am. Chem. Soc.* **127**, 14186–14187 (2005).
5. Manzuna Sapu, C., Bäckvall, J.-E. & Deska, J. Enantioselective enzymatic desymmetrization of prochiral allenic diols. *Angew. Chem. Int. Ed.* **50**, 9731–9734 (2011).
6. Sherry, B. D. & Toste, F. D. Gold(I)-catalyzed propargyl claisen rearrangement. *J. Am. Chem. Soc.* **126**, 15978–15979 (2004).
7. Pu, X. & Ready, J. M. Direct and stereospecific synthesis of allenes via reduction of propargylic alcohols with $Cp_2Zr(H)Cl$. *J. Am. Chem. Soc.* **130**, 10874–10875 (2008).
8. Uehling, M. R., Marionni, S. T. & Lalic, G. Asymmetric synthesis of trisubstituted allenes: copper-catalyzed alkylation and arylation of propargylic phosphates. *Org. Lett.* **14**, 362–365 (2012).
9. Wu, S., Huang, X. & Wu, W. A C-H bond activation-based catalytic approach to tetrasubstituted chiral allenes. *Nat. Commun.* **6**, 7946 (2015).
10. Ruchti, J. & Carreira, E. M. Rh-catalyzed stereospecific synthesis of allenes from propargylic benzoates and arylboronic acids. *Org. Lett.* **18**, 2174–2176 (2016).
11. Ogasawara, M. Catalytic enantioselective synthesis of axially chiral allenes. *Tetrahedron.: Asymmetry* **20**, 259–271 (2009).
12. Yu, S. & Ma, S. How easy are the syntheses of allenes? *Chem. Commun.* **47**, 5384–5418 (2011).
13. Neff, R. K. & Frantz, D. E. Recent advances in the catalytic syntheses of allenes: a critical assessment. *ACS Catal.* **4**, 519–528 (2014).
14. Ye, J. & Ma, S. Conquering three-carbon axial chirality of allenes. *Org. Chem. Front.* **1**, 1210–1224 (2014).
15. Shirakawa, S., Liu, S. & Kaneko, S. Organocatalyzed asymmetric synthesis of axially, planar, and helical chiral compounds. *Chem. Asian J.* **11**, 330–341 (2016).
16. Chu, W.-D., Zhang, Y. & Wang, J. Recent advances in catalytic asymmetric synthesis of allenes. *Catal. Sci. Technol.* **7**, 4570–4579 (2017).
17. Nishimura, T., Makino, H. & Nagaosa, M. Rhodium-catalyzed enantioselective 1,6-addition of arylboronic acids to enynamides: asymmetric synthesis of axially chiral allenylsilanes. *J. Am. Chem. Soc.* **132**, 12865–12867 (2010).
18. Wang, M., Liu, Z.-L. & Zhang, X. Synthesis of highly substituted racemic and enantioenriched allenylsilanes via copper-catalyzed hydrosilylation of (Z)-2-alken-4-ynoates with silylboronate. *J. Am. Chem. Soc.* **137**, 14830–14833 (2015).
19. Yao, Q., Liao, Y. & Lin, L. Efficient synthesis of chiral trisubstituted 1,2-allenyl ketones by catalytic asymmetric conjugate addition of malonic esters to enynes. *Angew. Chem. Int. Ed.* **55**, 1859–1863 (2016).
20. Imada, Y., Nishida, M. & Kutsuwa, K. Palladium-catalyzed asymmetric amination and imidation of 2,3-allenyl phosphates. *Org. Lett.* **7**, 5837–5839 (2005).
21. Wan, B. & Ma, S. Enantioselective decarboxylative amination: synthesis of axially chiral allenyl amines. *Angew. Chem. Int. Ed.* **52**, 441–445 (2013).
22. Wang, G., Liu, X. & Chen, Y. Diastereoselective and enantioselective alleno-aldol reaction of allenoates with isatins to synthesis of carbinol allenoates catalyzed by gold. *ACS Catal.* **6**, 2482–2486 (2016).
23. Crouch, I. T., Neff, R. K. & Frantz, D. E. Pd-catalyzed asymmetric β-hydride elimination en route to chiral allenes. *J. Am. Chem. Soc.* **135**, 4970–4973 (2013).
24. Li, Z., Boyarskikh, V. & Hansen, J. H. Scope and mechanistic analysis of the enantioselective synthesis of allenes by Rhodium-catalyzed tandem ylide formation/[2,3]-sigmatropic rearrangement between donor/acceptor carbenoids and propargylic alcohols. *J. Am. Chem. Soc.* **134**, 15497–15504 (2012).
25. Wang, Y., Zhang, W. & Ma, S. A room-temperature catalytic asymmetric synthesis of allenes with ECNU-Phos. *J. Am. Chem. Soc.* **135**, 11517–11520 (2013).
26. Liu, Y. et al. Nickel(II)-Catalyzed asymmetric propargyl and allyl Claisen rearrangements to allenyl- and allyl-substituted *β*-ketoesters. *Angew. Chem. Int. Ed.* **53**, 11579–11582 (2014).
27. Liu, Y. et al. Synergistic kinetic resolution and asymmetric propargyl claisen rearrangement for the synthesis of chiral allenes. *Angew. Chem. Int. Ed.* **55**, 4054–4058 (2016).
28. Xiao, Q., Xia, Y. & Li, H. Coupling of N-tosylhydrazones with terminal alkynes catalyzed by copper(I): synthesis of trisubstituted allenes. *Angew. Chem. Int. Ed.* **50**, 1114–1117 (2011).
29. Tang, Y., Chen, Q. & Liu, X. Direct synthesis of chiral allenoates from the asymmetric C-H insertion of α-diazoesters into terminal alkynes. *Angew. Chem. Int. Ed.* **54**, 9512–9517 (2015).
30. Chu, W.-D., Zhang, L. & Zhang, Z. Enantioselective synthesis of trisubstituted allenes via Cu(I)-catalyzed coupling of diazoalkanes with terminal alkynes. *J. Am. Chem. Soc.* **138**, 14558–14561 (2016).
31. Poh, J.-S., Makai, S. & Keutz, T. Rapid asymmetric synthesis of disubstituted allenes by coupling of flow-generated diazo compounds and propargylated amines. *Angew. Chem. Int. Ed.* **56**, 1864–1868 (2017).
32. Tang, X. et al. $CuBr_2$-catalyzed enantioselective routes to highly functionalized and naturally occurring allenes. *Org. Chem. Front.* **2**, 688–691 (2015).
33. Zhang, W., Zheng, S. & Liu, N. Enantioselective bromolac-tonization of conjugated (Z)-enynes. *J. Am. Chem. Soc.* **132**, 3664–3665 (2010).
34. Qian, H., Yu, X. & Zhang, J. Organocatalytic enantioselective synthesis of 2,3-allenoates by intermolecular addition of nitroalkanes to activated enynes. *J. Am. Chem. Soc.* **135**, 18020–18023 (2013).
35. Liu, H., Leow, D. & Huang, K.-W. Enantioselective synthesis of chiral allenoates by guanidine-catalyzed isomerization of 3-alkynoates. *J. Am. Chem. Soc.* **131**, 7212–7213 (2009).
36. Jiang, Y., Diagne, A. B. & Thomson, R. J. Enantioselective synthesis of allenes by catalytic traceless petasis reactions. *J. Am. Chem. Soc.* **139**, 1998–2005 (2017).
37. Hashimoto, T., Sakata, K. & Tamakuni, F. Phase-transfer-catalysed asymmetric synthesis of tetrasubstituted allenes. *Nat. Chem.* **5**, 240–244 (2013).
38. Mbofana, C. T. & Miller, S. J. Diastereo- and enantioselective addition of anilide-functionalized allenoates to N-acylimines catalyzed by a pyridylalanine-based peptide. *J. Am. Chem. Soc.* **136**, 3285–3292 (2014).
39. Tap, A., Blond, A. & Wakchaure, V. N. Chiral allenes via alkynylogous mukaiyama aldol reaction. *Angew. Chem. Int. Ed.* **55**, 8962–8965 (2016).
40. Qian, D., Wu, L. & Sun, J. Organocatalytic synthesis of chiral tetrasubstituted allenes from racemic propargylic alcohols. *Nat. Commun.* **8**, 567 (2017).
41. Kumar, S., Bawa, S. & Gupta, H. Biological activities of quinoline derivatives. *Mini Rev. Med Chem.* **14**, 1648–1654 (2009).
42. Tian, S., Chen, Y. & Huang, J. Asymmetric organic catalysis with modified cinchona alkaloids. *Acc. Chem. Res.* **37**, 621–631 (2004).
43. Chen, G., Zhuang, G. & Li, G. Ligand-enabled β-C-H arylation of α-amino acids without installing exogenous directing groups. *Angew. Chem. Int. Ed.* **56**, 1506–1509 (2017).
44. Cornelissen, L., Lefrancq, M. & Riant, O. Copper-catalyzed cross-coupling of vinylsiloxanes with bromoalkynes: synthesis of enynes. *Org. Lett.* **16**, 3024–3027 (2014).
45. Miki, Y., Hirano, K. & Miura, M. Copper-catalyzed intermolecular regioselective hydroamination of styrenes with polymethylhydrosiloxane and hydroxylamines. *Angew. Chem. Int. Ed.* **52**, 10830–10834 (2013).
46. Yang, Y., Shi, S.-L. & Niu, D. Catalytic asymmetric hydroamination of unactivated internal olefins to aliphatic amines. *Science* **349**, 62–66 (2015).
47. Niu, D. & Buchwald, S. L. Design of modified amine transfer reagents allows the synthesis of α-chiral secondary amines via CuH-catalyzed hydroamination. *J. Am. Chem. Soc.* **137**, 9716–9721 (2015).
48. Xi, Y., Butcher, T. W., Zhang, J. & Hartwig, J. F. Regioselective, asymmetric formal hydroamination of unactivated internal alkenes. *Angew. Chem. Int. Ed.* **55**, 776–780 (2016).
49. Han, J. T., Jang, W. J., Kim, N. & Yun, J. Asymmetric synthesis of borylalkanes via copper-catalyzed enantioselective hydroallylation. *J. Am. Chem. Soc.* **138**, 15146–15149 (2016).
50. Zhou, Y., Bandar, J. S. & Buchwald, S. L. Enantioselective CuH-catalyzed hydroacylation employing unsaturated carboxylic acids as aldehyde surrogates. *J. Am. Chem. Soc.* **139**, 8126–8129 (2017).
51. Xi, Y. & Hartwig, J. F. Mechanistic studies of copper-catalyzed asymmetric hydroboration of alkenes. *J. Am. Chem. Soc.* **139**, 12758–12772 (2017).
52. Rendler, S. & Oestreich, M. Polishing a diamond in the rough: "Cu-H" catalysis with silanes. *Angew. Chem. Int. Ed.* **46**, 498–504 (2007).
53. Deutsch, C., Krause, N. & Lipshutz, B. H. CuH-catalyzed reactions. *Chem. Rev.* **108**, 2916–2927 (2008).
54. Pirnot, M. T., Wang, Y.-M. & Buchwald, S. L. Copper hydride catalyzed hydroamination of alkenes and alkynes. *Angew. Chem. Int. Ed.* **55**, 48–57 (2016).
55. Meng, F., Haeffner, F. & Hoveyda, A. H. Diastereo- and enantioselective reactions of bis(pinacolato)diboron, 1,3-enynes, and aldehydes catalyzed by an easily accessible bisphosphine-Cu complex. *J. Am. Chem. Soc.* **136**, 11304–11307 (2014).
56. Yang, Y., Perry, I. B. & Buchwald, S. L. Copper-catalyzed asymmetric addition of olefin-derived nucleophiles to ketones. *Science* **353**, 144–150 (2016).
57. Huang, Y., del Pozo, J. & Hoveyda, A. H. Enantioselective synthesis of trisubstituted allenyl-B(pin) compounds by phosphine-Cu-catalyzed 1,3-enyne hydroboration. insights regarding stereo-chemical integrity of Cu-allenyl intermediates. *J. Am. Chem. Soc.* **140**, 2643–2655 (2018).
58. Sang, H. L., Yu, S. & Ge, S. Copper-catalyzed asymmetric hydroboration of 1,3-enynes with pinacolborane to access chiral allenylboronates. *Org. Chem. Front.* **5**, 1284–1287 (2018).
59. Gao, D.-W., Xiao, Y. & Engle, K. M. Catalytic, enantioselective synthesis of allenyl boronates. *ACS Catal.* **8**, 3650–3654 (2018).

60. Yu, S., Sang, H. L. & Ge, S. Enantioselective copper-catalyzed alkylation of quinoline N-oxides with vinylarenes. *Angew. Chem. Int. Ed.* **56**, 15896–15900 (2017).
61. Grandclaudon, C., Michelet, V. & Toullec, P. Y. Synthesis of polysubstituted 2-iodoindenes via iodonium-induced cyclization of arylallenes. *Org. Lett.* **18**, 676–679 (2016).
62. Andersson, H., Gustafsson, M. & Bostrom, D. The regio- and stereoselective synthesis of trans-2,3-dihydropyridine N-oxides and piperidines. *Angew. Chem. Int. Ed.* **48**, 3288–3291 (2009).
63. Larionov, O. V., Stephens, D. & Mfuh, A. Direct, catalytic, and regioselective synthesis of 2-alkyl-, aryl-, and alkenyl-substituted N-heterocycles from N-oxides. *Org. Lett.* **16**, 864–867 (2014).
64. Bandar, J. S., Pirnot, M. T. & Buchwald, S. L. Mechanistic studies lead to dramatically improved reaction conditions for the Cu-catalyzed asymmetric hydroamination of olefins. *J. Am. Chem. Soc.* **137**, 14812–14818 (2015).

Acknowledgements

This work was supported by the grant from NUS Young Investigator Award (R-143-000-630-133) and the Ministry of Education of Singapore (R-143-000-A07-112). Computational study was supported by the National Natural Science Foundation of China (21702128) and calculations were performed on high-performance computing system at Department of Chemistry, Zhejiang University.

Author contributions

S.Y. planned and conducted most of the experiments; S.Y. and H.L.S. prepared substrates for the reaction scope evaluation; S.-Q.Z. and X.H. conducted DFT calculation studies. S.G. directed the projects and S.G., S.Y., and X.H. co-wrote the manuscript. All authors contributed to the discussion.

Additional information

Supplementary information accompanies this paper at https://doi.org/10.1038/s42004-018-0065-4.

Competing interests: The authors declare no competing interests.

Reprints and permission information is available online at http://npg.nature.com/reprintsandpermissions/

Publisher's note: Springer Nature remains neutral with regard to jurisdictional claims in published maps and institutional affiliations.